Coastal water vapor isotopic composition driven by katabatic wind variability in summer at Dumont 1 d'Urville, coastal East Antarctica

Camille Bréant, Christophe Leroy dos Santos, Cécile Agosta, Mathieu Casado, Elise Fourré, Sentia Goursaud, Valérie Masson-Delmotte, Vincent Favier, Olivier Cattani, Frédéric Prié, et al.

Coastal water vapor isotopic composition driven by katabatic wind variability in summer at Dumont d'Urville, coastal East Antarctica

Camille Bréant[1], Christophe Leroy Dos Santos[1], Cécile Agosta[1,2], Mathieu Casado[1], Elise Fourré[1], Sentia Goursaud[1], Valérie Masson-Delmotte[1], Vincent Favier[2], Olivier Cattani[1], Frédéric Prié[1], Benjamin Golly[2], Anaïs Orsi[1], Patricia Martinerie[2], Amaëlle Landais[1,]*

[1] Laboratoire des Sciences du Climat et de l'Environnement (LSCE) - IPSL, UMR 8212, CEA-CNRS-UVSQ, Université Paris-Saclay, F-91190 Gif sur Yvette, France

[2] Univ. Grenoble Alpes, CNRS, IRD, Grenoble INP, Institut de Géophysique de l'Environnement (IGE), F-38000 Grenoble, France

[*] corresponding author : amaelle.landais@lsce.ipsl.fr

Abstract

Dumont d'Urville station, located on the East coast of Antarctica in Adélie Land, is in one of the windiest coastal region on Earth, due to katabatic winds downslope from the East Antarctic ice sheet. In summer, the season of interest in this study, coastal weather is characterized by well-marked diel cycles in temperature and wind patterns. Our study aims at exploring the added value of water vapor stable isotopes in coastal Adélie Land to provide new information on the local atmospheric water cycle and climate. An important application is the interpretation of water isotopic profiles in snow and ice cores recently drilled in Adélie Land. We present the first continuous measurements of $\delta^{18}O$ and d-excess in water vapor over Adélie Land. During our measurements period (26/12/2016 to 03/02/2017), we observed clear diel cycles in terms of temperature, humidity and isotopic composition. The cycles in isotopic composition are particularly large given the muted variations in temperature when compared to other Antarctic sites where similar monitoring have been performed. Based on data analyses and simulations obtained with the regional MAR model on the coastal Adélie Land, we suggest that the driver for $\delta^{18}O$ and d-excess diel variability in summer at Dumont d'Urville is the variations of the strength of the wind coming from the continent: the periods with strong wind are associated with the arrival of relatively dry air with water vapor associated with low $\delta^{18}O$ and high d-excess from the Antarctic plateau. Finally, in addition to the interpretation of snow and ice core isotopic profiles in the coastal regions, our study has implications for the evaluation of atmospheric models equipped with water isotopes.

1. Introduction

Adélie Land, located on the coast of Antarctica, in the Indian Ocean sector (Figure 1) is one of the windiest coastal regions on Earth, due to katabatic winds blowing downslope from the East Antarctic Plateau (Pettré et al., 1993; Wendler et al., 1997; König-Langlo et al., 1998). This region is also associated with a coastal winter polynya playing a key role on sea ice formation, deep water formation, and associated food webs (Kusahara et al., 2017). Large variations of regional sea ice extent have been monitored since 1979 (Massom et al., 2013), with maximum expansion of pack ice up to 300 km from the coast (Massom & Stammerjohn, 2010; Tamura et al., 2016). Sea ice may persist during summer months (Smith et al., 2011). Located at (66°39'S, 140°00 E) in Adélie Land, the Dumont d'Urville station (hereafter DDU) has provided continuous weather monitoring since 1957 (Périard & Pettré, 1993). In summer, the season of interest in this study, coastal weather is in general characterized by well-marked diel cycles in temperature and wind patterns, associated with the contrasted influence of katabatic winds during night time and frequent upslope sea breezes during day time (Gallée & Pettré, 1998). Recent monitoring studies in coastal Adélie Land have evidenced the importance of blowing snow as well as snow sublimation processes induced by local atmospheric dynamic for the regional surface mass balance of the Antarctic ice sheet (Barral et al., 2014; Amory et al., 2015; Grazioli et al., 2017). As an example, the recent study of Grazioli et al. (2017) suggests that low-level sublimation linked to katabatic winds can lead to a 35% reduction of snowfall on the East Antarctic coast and to a 17% reduction when considering whole Antarctica. One objective of our study is thus the need to better document and understand the processes affecting atmospheric moisture transport and snow-air exchanges in coastal polar areas with climatic conditions comparable to Adélie Land.

Here, we explore the added value of water isotopes to document the local and regional atmospheric water cycle through presentation of new stable isotopic measurements on water vapor performed in the summer season during 40 days at DDU near the surface. Water stable isotopes are integrated tracers of the atmospheric water cycle, as equilibrium and kinetic fractionation leave an imprint of each process occurring along the moisture path: evaporation, atmospheric moisture transport, and condensation (Jouzel, 2013). In Antarctic ice cores, water stable isotopes are amongst the core classical measurements. In high accumulation regions, they are combined with ice core chemistry measurements to identify seasonal cycles and develop ice core layer counted chronologies (e.g. Roberts et al., 2015; Thomas et al., 2017). In central Antarctic regions, the variability of water stable isotopes ($\delta^{18}O$ or δD) in precipitation is dominated by a fingerprint of local temperature variability at daily, seasonal and inter-annual scales (Stenni et al., 2016). In contrast to sites located on the East Antarctic plateau where the temperature-driven distillation effect is more important than oceanic source effects on precipitation water isotopic variations (e.g. Touzeau et al., 2016), the climatic

interpretation of water isotopic composition in coastal regions is more ambiguous (e.g. Altnau et al., 2014; Goursaud et al., 2016). Indeed, the influence of the origin of precipitation on water isotopes composition is probably more important in coastal regions than in the Antarctic plateau (Jouzel et al., 2013). In addition, in coastal areas characterized by intense winds, deposition effects linked to sublimation of falling snow and post-deposition effects linked with remobilization of surface snow (e.g. blowing snow) are expected to alter the snow isotopic composition, hence complicating the climatic interpretation of the water stable isotope variability (e.g. Landais et al., 2017). Finally, isotopic composition can be affected by microphysical processes in clouds and precipitation (Moore et al., 2016) and summer precipitation at DDU can be significantly rimed (Grazioli et al., 2017) which has an effect on the isotopic composition of precipitation. Recently, one 22.4 m ice core spanning the period 1946-2006 was retrieved 10.24 km far from DDU. Decadal variations in $\delta^{18}O$ are parallel to decadal variations in DDU surface air temperature (Goursaud et al., 2017), but sub-decadal variations remain unexplained and could arise from variations in moisture origin as well as deposition or post-deposition "noise", calling for water isotope measurements in the vapor to decipher the processes at play at the scale of weather events. Our study thus aims at providing bases for the interpretation of snow and ice core in Adélie Land in terms of past climate and water cycle dynamic. This is particularly relevant in the context of the project ASUMA (Improving the Accuracy of the SUrface Mass balance of Antarctica, 2014 – 2019) which recently enabled collection of numerous 20 – 40 m snow cores in the coastal Adélie Land.

Recent studies have used continuous monitoring of water stable isotopes in surface water vapour and surface snow in Antarctica to explore the influences of both atmospheric dynamic and post-deposition effects on surface snow isotopic composition (Casado et al., 2016; Ritter et al., 2016). These studies have evidenced patterns of diel variations, and demonstrated that the surface snow isotopic composition can change in-between precipitation events in parallel with changes in vapour isotopic composition, itself driven by changes in atmospheric advection patterns, as initially observed above the Greenland ice sheet (Steen-Larsen et al., 2014). Diel variations in surface vapour isotopic composition were also reported in summer in polar regions with no snow cover, for instance in Kangerlussuaq, West Greenland (Kopec et al., 2014). In this site, the diel variations were attributed to local boundary layer characteristics involving sea breeze processes. Day to day surface vapour isotopic variations monitored from a ship were also related to shifts in very local atmospheric circulation patterns near Syowa, on the East Antarctic coast (e.g. Kurita et al., 2016a; Kurita et al., 2016b).

Summarizing, our study is motivated by the need to better understand the drivers of water vapour isotope variations in Adélie Land for (i) ice core interpretation, (ii) exploring the added value of water stable isotopes to provide new information on the local atmospheric moisture budget and thus (iii) improving our knowledge of the present and recent coastal climate and water cycle variations. This is

relevant for the regional surface mass balance of the ice sheet as well as for the evaluation of atmospheric models equipped with water isotopes. We have thus implemented a laser spectroscopy instrument to measure continuously the isotopic composition of water vapor at DDU during summer 2016-2017, taking advantage of the excellent facilities of the station.

This paper is organized as follows. We first report (Section 2) the experimental set up, as well as the calibration of the isotopic measurements to provide continuous $\delta^{18}O$ and d-excess measurements in the water vapor at DDU during 40 days. The analysis of the calibrated dataset (Section 3) depicts different periods of measurements based on weather conditions, especially wind regimes, sky conditions and one snowfall event. The unequivocal isotopic diel cycles in DDU surface water isotopes are characterized in terms of amplitude and timing (Section 4) and compared with local meteorological data as well as diel cycles observed in continuous water vapor $\delta^{18}O$ time series in other polar regions. We then summarize our key findings and suggest ways forward (Section 5).

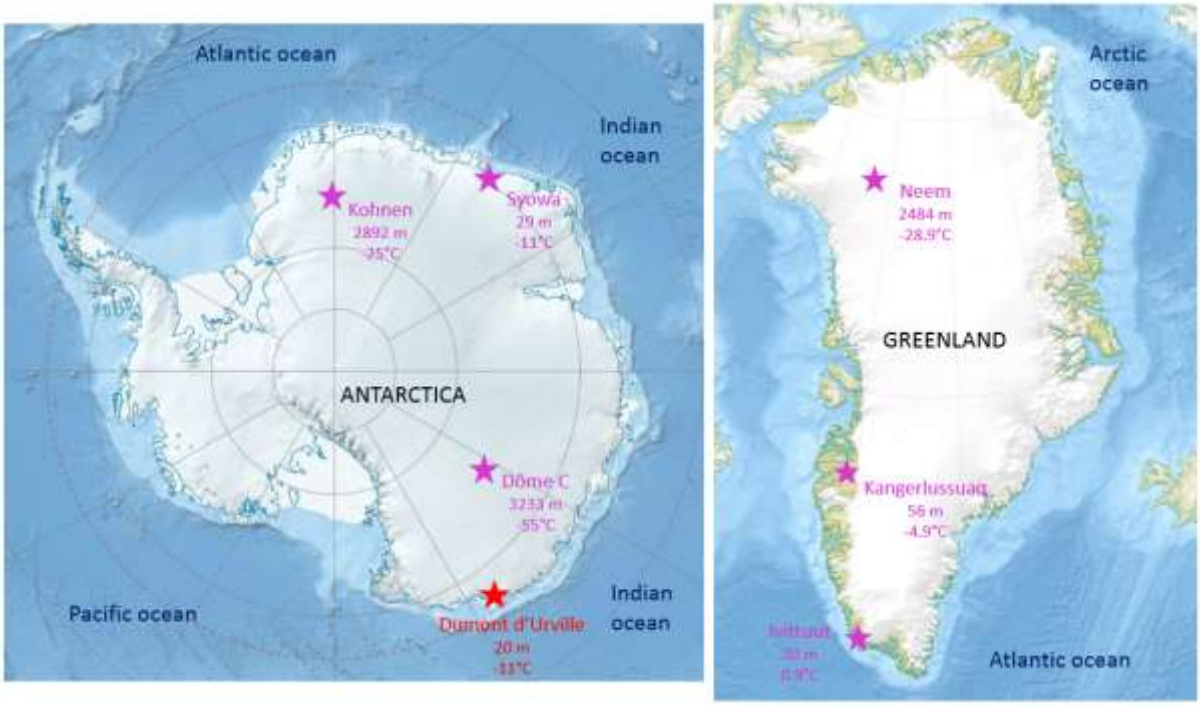

Figure 1: Maps of Antarctica (left) and Greenland (right) showing the location of our study site (red) and the location of other sites where continuous water stable isotope records have provided insights on diel variations (pink). For each site, height and near-surface mean annual temperature are given.

2. Analytical method

We installed a PICARRO Li-2130 laser spectroscopy in the "Laboratoire 3" shelter, located on the inland side of DDU station (Figure 2). A 6 m length heated copper tube has been deployed to continuously sample water vapor at 2 m above the ground. The extremity of the tube was covered by a Gelman Zefluor 0.5 μm filter to prevent the inflow of precipitation or blowing snow. Continuous

measurements of water vapor isotopic composition took place during 40 days from December 26th 2016 to February 3rd 2017. Except for one electrical shutdown on January 4th 2017, the only interruptions of our monitoring occurred during bi-daily calibrations.

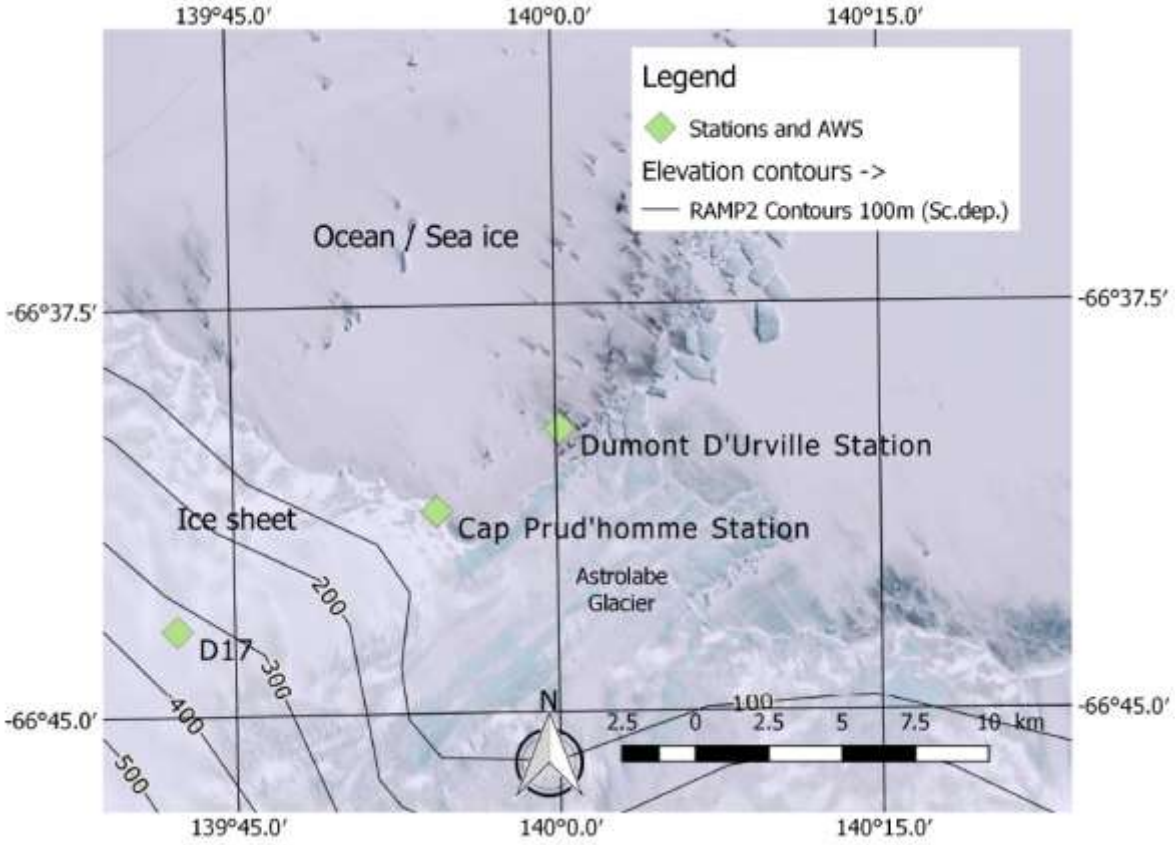

Figure 2: Map of DDU station showing the location of the two AWS installed at Cap Prud'homme and D17. Background image is a 15-m resolution Landsat Image Mosaic of Antarctica from the area taken between 1999-2002 (Bindschadler et al., 2008). Elevation lines are extracted from the digital elevation model from Radarsat Antarctic Mapping Project Digital Elevation Model Version 2 (RAMP2, Liu et al., 2001). The map was designed with Quantarctica3 (https://www.qgis.org/fr/site/about/case_studies/antarctica.html).

During our monitoring period, the volume water vapour mixing ratio (referred to as humidity in the following) varied between 2000 and 6000 ppmv (or 1.244 to 3.732 $g.kg^{-1}$). The raw $\delta^{18}O$ values varied typically between -23 and -35‰ (Figure 3). The procedure for calibration of the raw data is detailed in supplementary online material (SOM). Despite problems with the calibration module during the first weeks after installation (default in the electrical powering of the instrument), we applied as much as possible the corrections proposed in previous studies as follows (see also SOM). We corrected the raw laser spectroscopy $\delta^{18}O$ measurements for (1) the influence of humidity on $\delta^{18}O$ and δD values, (2) shifts between measured $\delta^{18}O$ (δD) and true $\delta^{18}O$ (δD) values and (3) the temporal drift of the instrument for $\delta^{18}O$ and δD (Tremoy et al., 2012; Steen-Larsen et al., 2013). The uncertainties on the isotopic measurements mainly result from scattering of the calibration points as well as missing

calibration points during several weeks. The upper limits of uncertainties on the absolute values of $\delta^{18}O$ and d-excess (δD-8*$\delta^{18}O$) vary respectively between 1‰ and 3.5‰ and between 5‰ and 25‰.

This uncertainty, mainly linked to unknown drift because of calibration issues during this field season, should be applied on the absolute values of $\delta^{18}O$ and d-excess but not on their short-term variations at the timescale of a few days. In the following sections of this manuscript, we thus do not discuss much the absolute values of $\delta^{18}O$ and d-excess but rather focus on the short-term (diel) variability.

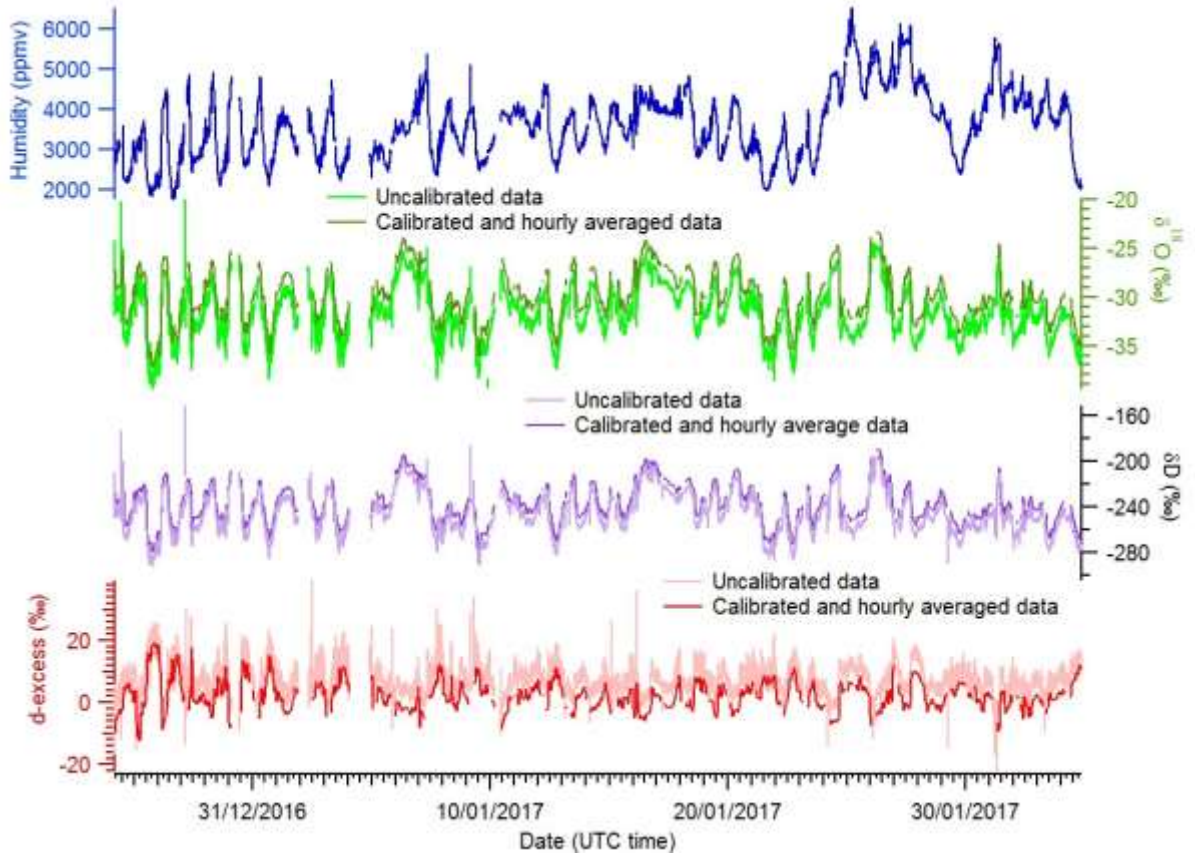

<u>Figure 3</u>: Humidity (blue), $\delta^{18}O$ (green), δD (violet) and d-excess (δD-8$\delta^{18}O$, red) measured by the laser spectroscopy instrument at DDU. Raw data (initial resolution of one second but averaged over one minute here) are shown in light green, light violet and light red for $\delta^{18}O$, δD and d-excess respectively. Calibrated $\delta^{18}O$, δD and d-excess data (hourly resolution) are shown in dark green, dark violet and red, respectively.*

The DDU weather station provides continuous measurements at hourly resolution. Temperature and humidity are measured from a Vaisala HMP 110 probe in a standard meteorological shelter, 1.5 m above the ground surface. Wind speed and direction are measured on a 10 m tower located a few meters from the meteorological shelter. Surface wind directions can be used to separate between winds with continental origin and winds with oceanic origins. Jourdain (2001) and Angot et al. (2016)

identified oceanic winds at DDU in the range from 270 to 110°, the other winds having a continental origin.

January 2017 is a relatively warm month with a mean monthly air temperature of -0.4°C, compared to a mean January temperature of -0.9 °C (±0.9°C) over the whole 1957 -2017 record, though not extreme (a mean air temperature of 1°C was recorded in January 1972 and 2010). In January 2017, the sea ice extent around DDU is among the three largest summer sea ice extents observed around DDU (with January 2012 and January 2013) over the last 44 years, as estimated from the Hadley Center Sea Ice and Sea Surface Temperature data set HadISST.2 (Titchner & Rayner, 2014), comparable to the sea ice extent observed in January 2012 and 2013. Even though a direct causal link has not been proven with sea ice extent, we note that the January 2017 Southern Annular Mode index is unusually low, showing the lowest value since 1993, and the 5th lowest value since 1984 (Marshall, 2003).

In addition, for this study we used the meteorological data recorded by the automated weather station (AWS) set up at Cap Prud'homme (66.688°S, 139.907°E, 5 km from Dumont d'Urville on the continent, 27 m above sea level, Figure 2). The sensor characteristics are listed in Favier et al. (2011). Quantities were recorded as half-hourly means of measurements performed at 10 s time intervals. In addition to the temperature, humidity and wind characteristics, this dataset also displays radiative data (e.g. incoming shortwave and longwave fluxes, outgoing longwave flux).

The data obtained at DDU and at Cap Prud'homme are well correlated at the hourly scale over the whole period of measurements with the same amplitude of the signal (Figure 4). The temperature and wind speed data from Cap Prud'homme are very useful data for our study because (1) they were obtained on the continent, in an area more directly influenced by the katabatic winds, and (2) the data are less affected by buildings on the station as in DDU. Finally, note that the Cap Prud'homme data are obtained at a highest resolution so that they are often preferred compared to the DDU data.

3. Results

Figure 4 displays our 40-day record of DDU water vapor isotopic composition in parallel with temperature, humidity, wind speed, wind direction and incoming short- and longwave fluxes, the latter indicating the cloud coverage. The time series for water vapor isotopic composition are overall well correlated with humidity and temperature (see Table 1). While we do not comment on the long term trends of the water isotopic compositions because of calibration issues reported above, we note that humidity measured with the same instrument and validated by other sensors reaches high levels (above 5000 ppmv) during the period between January 25th and 28th, corresponding to the longest

snowfall event of the monitoring period. This period is also associated with high incoming longwave flux showing radiation as expected under wet and cloudy conditions. Wind speed does not exhibit much long term variability (i.e. at the timescale of a few days/weeks) except for a period with almost no wind between the 16th and the 18th of January and periods of strong winds at the end of January / beginning of February when cloudy conditions prevail.

At shorter timescales, we observe strong diel cycles in δD, $\delta^{18}O$, temperature, humidity, and wind characteristics. The diel variations in wind direction are however beyond detectability in the case of very low wind speeds (i.e. below 3 m.s^{-1} such as between the 16th and the 18th of January with also no variation in the other climatic variables in this case confirming that the absence of signal in the wind direction is a physical signal). The most reliable wind direction is the one measured when wind speed is larger than 5 m.s^{-1}: in this case, wind has a continental origin and displays katabatic characteristics (SOM). The northward wind direction with relatively weak wind is less reliable. Diel cycles of $\delta^{18}O$, temperature, humidity, wind speed and d-excess are visible almost over the whole period. We nevertheless observe a strong variability on the amplitude of the different cycles. As examples, maximal (minimal) amplitudes of diel cycles in $\delta^{18}O$, temperature and humidity are respectively 11.5‰ (0.9‰), 8°C (1°C), 2640 ppmv (280 ppmv).

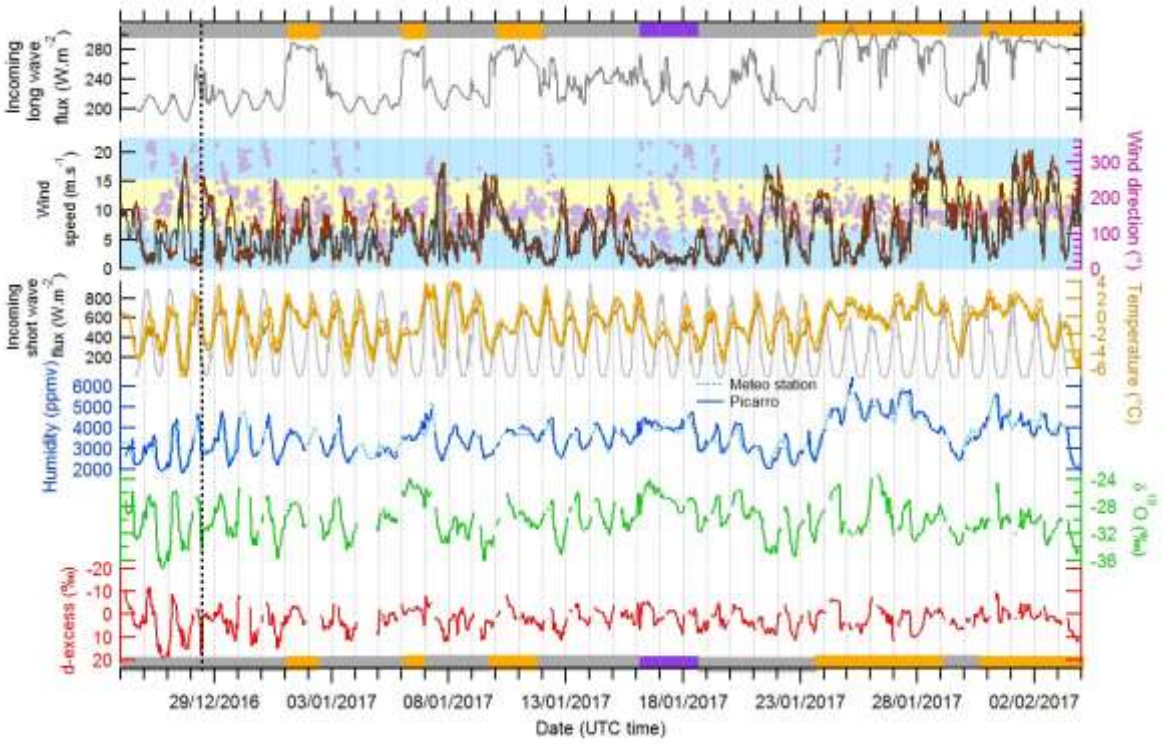

Figure 4: Evolution of incoming long wave flux (used here to differentiate cloudy from clear sky conditions), wind strength (bordeaux), wind direction (purple dots) and temperature (orange) from the Cap Prud'homme automatic weather station. Evolution of temperature (light orange), wind speed (black) and humidity from DDU meteorological station together with the evolution of humidity, $\delta^{18}O$

and d-excess (inverted axis) from DDU Picarro instrument. In the second upper panel, the horizontal blue and yellow bands stand for the range of direction winds originating from the ocean or from the continent respectively. The grey, orange and violet rectangles indicate the periods with different weather conditions (clear sky, cloudy, no wind). The snowy period (25th to 28th of January 2017) is included in the cloudy periods. The dashed vertical line corresponds to a specific event discussed in section 4.

We have clustered our measurements based on the weather conditions in periods with clear sky (grey on Figure 4), cloudy conditions (orange on Figure 4) and no wind conditions (violet on Figure 4, corresponding to days without katabatic wind occurrence even during the night). During the period without wind, only a small diel cycle is observed in the temperature record but no clear diel cycles are observed in the humidity and $\delta^{18}O$ records. During the clear sky periods, clear diel cycles are observed in temperature (mean amplitude of 4.5°C), humidity (mean amplitude of 1300 ppmv), $\delta^{18}O$ (mean amplitude of 5.4 ‰), d-excess (mean amplitude of 10 ‰) and wind speed (mean amplitude of 7 m.s^{-1}) (Figure 5a). In most cases, there are significant correlations (Table 1) between temperature, humidity and $\delta^{18}O$ while both d-excess and wind speed are significantly anti-correlated with these 3 parameters. However, the correlation between $\delta^{18}O$ and near surface temperature diel cycles is surprisingly low (R^2=0.24), given the relationship between temperature, atmospheric distillation and isotopic depletion leading to a strong correlation (R^2=0.9) on the Antarctic plateau between near surface temperature and $\delta^{18}O$ of precipitation or surface snow along transects (Touzeau, et al., 2016; Stenni et al., 2016; Masson-Delmotte et al., 2008). When extracting the typical average diel cycles for the 5 parameters mentioned above (Figure 5a), we do not observe significant temporal shift between the maxima / minima in each record: temperature maximum is synchronous with minimum in wind speed, maximum in $\delta^{18}O$, maximum in humidity and minimum in d-excess. During the cloudy periods, diel cycles are less marked and the (anti-)correlations between the different parameters are much less clear (Figure 5b). In this case, we note a correlation between temperature and humidity as well as an anti-correlation between $\delta^{18}O$ and d-excess.

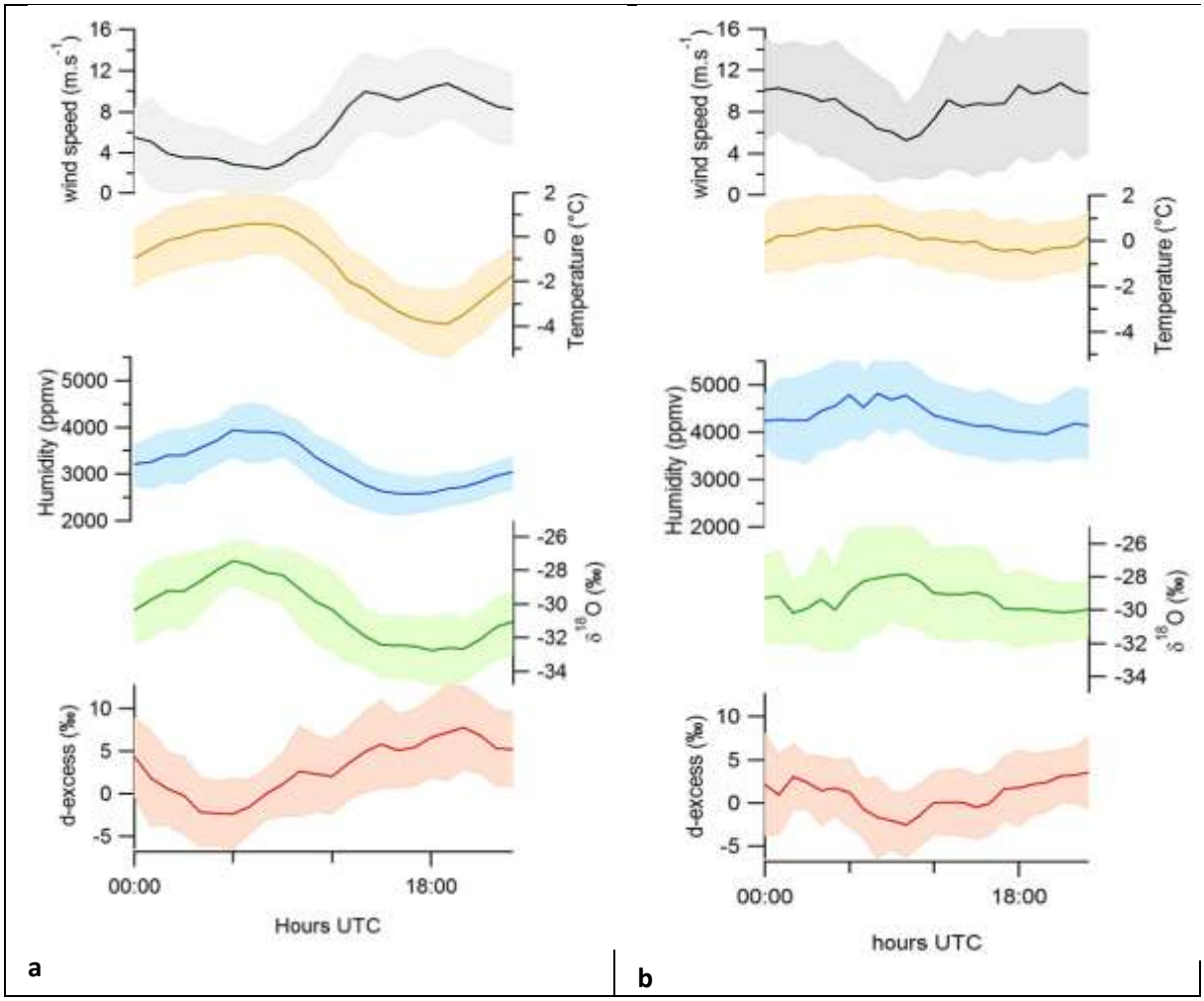

Figure 5: Average diel cycles of wind speed, temperature, humidity, $\delta^{18}O$ and d-excess during periods with clear sky conditions (a) and cloudy conditions (b) (see Figure 4 for identification of these time periods). The hourly data for the two different periods were averaged to produce the respective mean diel cycles. The envelopes in light colors were obtained from the standard deviation of the data obtained over the different days within each period. The time zone at DDU is UTC+ 10.

Periods / Variables	Clear Sky	Cloudy
d-excess vs temperature	0.18 (-6 ‰.K^{-1})	0.01
humidity vs temperature	0.49 (221 ppmv.K^{-1})	0.32
$\delta^{18}O$ vs temperature	0.24 (0.39 ‰.K^{-1})	0.11
d-excess vs $\delta^{18}O$	0.73 (-0.42)	0.56
$\delta^{18}O$ vs humidity	0.73 (0.003 ‰.$ppmv^{-1}$)	< 0.01
d-excess vs humidity	0.51 (-0.42 ‰.$ppmv^{-1}$)	< 0.01
Wind speed vs temperature	0.27 (1.1 $m.s^{-1}.K^{-1}$)	0.05
Humidity vs wind speed	0.36 (-244 $ppmv.s.m^{-1}$)	0.09
$\delta^{18}O$ vs wind speed	0.36 (-0.34 ‰.$s.m^{-1}$)	0.11
d-excess vs wind speed	0.11 (-0.42 ‰.$s.m^{-1}$)	< 0.01

Table 1: Correlation coefficients (R^2) between different climatic and/or isotopic parameters during the clear sky and cloudy periods at DDU based on hourly data (N=505 for clear sky periods; N=289 for cloudy periods). The slope between the two parameters is also reported within brackets for clear sky conditions when correlation and anti-correlation coefficients are at the highest. Note that although wind speed and d-excess appear correlated on figure 5b on an average diel cycle, this is not the case when taking all the individual data from the cloudy period.

4. Discussion

4-1- Drivers of the diel variations of the isotopic composition

The relatively low correlation between temperature and $\delta^{18}O$ even during the clear sky conditions rules out local air temperature as the main driver of vapor $\delta^{18}O$ diel variations. The correlation is much stronger between $\delta^{18}O$ and humidity variations for clear sky conditions (R^2=0.73, N=505). Two explanations can be proposed for driving these common variations at this stage: snow sublimation from the surface and advection and mixing in the atmosphere. In order to decipher these effects, we performed a comparison with outputs from the Modèle Atmosphérique Régional MAR (v3.6.4) forced by ERA-Interim over the Antarctic ice sheet at a 35 km horizontal resolution for the period of measurements (Agosta et al., 2019 extended to the years 2016 and 2017 for this study). A comparison

of the temperature, wind speed and humidity measurements with the corresponding series obtained by the model in the grid cell containing DDU (SOM) shows that this model is adapted to study the atmospheric dynamic at the diel scale in this site, and particularly the variations of humidity (SOM). The model enables us to disentangle the relative contribution of the local source of humidity from surface sublimation (surface turbulent moisture flux) to the variations of humidity related to horizontal air advection and the vertical turbulent moisture flux (mixing) according to the continuity equation applied to the water vapor in the atmospheric boundary layer (Garratt, 1994, equation 4):

$$\frac{\partial q}{\partial t} = -\mathbf{u} \cdot \nabla q - \nabla \cdot \mathbf{E} \quad \text{equation (1)}$$

where $\frac{\partial q}{\partial t}$ is the rate of change of specific humidity q (kg kg^{-1} s^{-1}) over time *t* (s), $-\mathbf{u} \cdot \nabla q$ is the advection of water vapor by the wind **u** (m s^{-1}), and $-\nabla \cdot \mathbf{E}$ is the divergence of the turbulent moisture flux **E** (kg kg^{-1} m s^{-1}). We neglect source and sink of humidity by condensation and sublimation in the atmosphere, as we focus on clear sky days when the atmosphere is undersaturated and blowing snow absent (see below). The advection term is dominated by the horizontal component, whereas the divergence of the turbulent moisture flux is dominated by the vertical component. Fig. 6 shows that the decrease in humidity is driven by the horizontal advection of dry continental air during the night, when the katabatic wind forms and strengthens, while the vertical turbulent mixing with the upper atmosphere drives the increase in humidity. The contribution of surface sublimation to the increase in humidity is one order of magnitude lower that the contribution of upper air mixing.

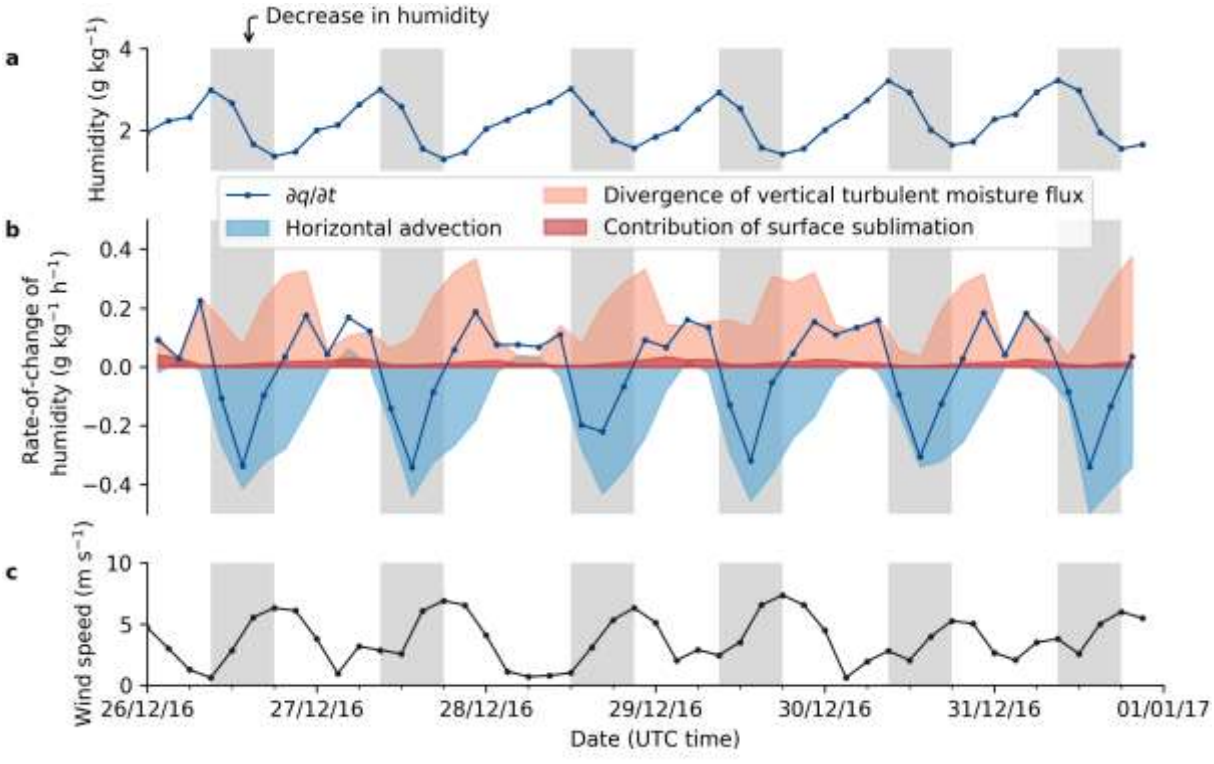

***Figure 6**: (a) Humidity, (b) rate-of-change of humidity (blue line), and (c) wind speed in MAR surface atmospheric layer (0-2 m) during clear sky days, in average for 3 h time steps. In (b), the contributions to the rate of change of humidity are displayed in plain color : the horizontal advection in light blue and the divergence of vertical turbulent moisture flux in light red (first and second terms of the right hand side of equation 1). The contribution of surface sublimation to the rate-of-change of humidity, which is a component of the divergence of vertical turbulent moisture flux, is shaded in red. Grey bands show periods when humidity decreases (negative rate of change of humidity in panel b).*

The proposed mechanism linking wind speed, humidity and water isotopic composition at the diel scale at DDU is the following. The continental temperature above DDU region exhibits a diel cycle linked to the decrease of incoming shortwave between 6:00 UTC and 18:00 UTC (Figure 5a). During this period, the radiative cooling at the surface of continental slopes induces the establishment of a strong katabatic flow that advects dry and cold air from the continent to the coastal region. The water vapor advected by these strong continental winds is characterized by low $\delta^{18}O$ and high d-excess since surface snow $\delta^{18}O$ has been shown to decrease and d-excess to increase from the coast to inland Antarctica (e.g. Masson-Delmotte et al., 2008; Touzeau et al., 2016). We thus propose that katabatic dynamics around DDU has a key role in driving diel cycles. This is particularly true during clear sky summer conditions when the radiative cooling is the strongest.

During cloudy period, diel temperature variations are muted (Figure 5b). The wind speed cycles are also less systematic over this period with days associated with relatively strong wind (e.g. beginning of February). During the arrival of a low pressure system at DDU (as observed between the 25th and the 28th of January), higher wind speed is correlated with higher humidity (and with $\delta^{18}O$ to a lesser extent) and with the occurrence of precipitation events (Figure 7). This can be interpreted as a significant proportion of marine air entering in the system. Sublimation during precipitation events may also contribute to explain the increase in $\delta^{18}O$ since the few maxima in $\delta^{18}O$ occur in most cases during precipitation events or the presence of virga. The time series is however too short to enable a firm conclusion based on a robust statistical approach. During this period, the anti-correlation between $\delta^{18}O$ and d-excess is preserved, as also observed during cloudy and clear sky conditions. Only with very weak surface winds (lower than 3 $m.s^{1}$) does the anti-correlation between $\delta^{18}O$ and d-excess at the diel scale disappear.

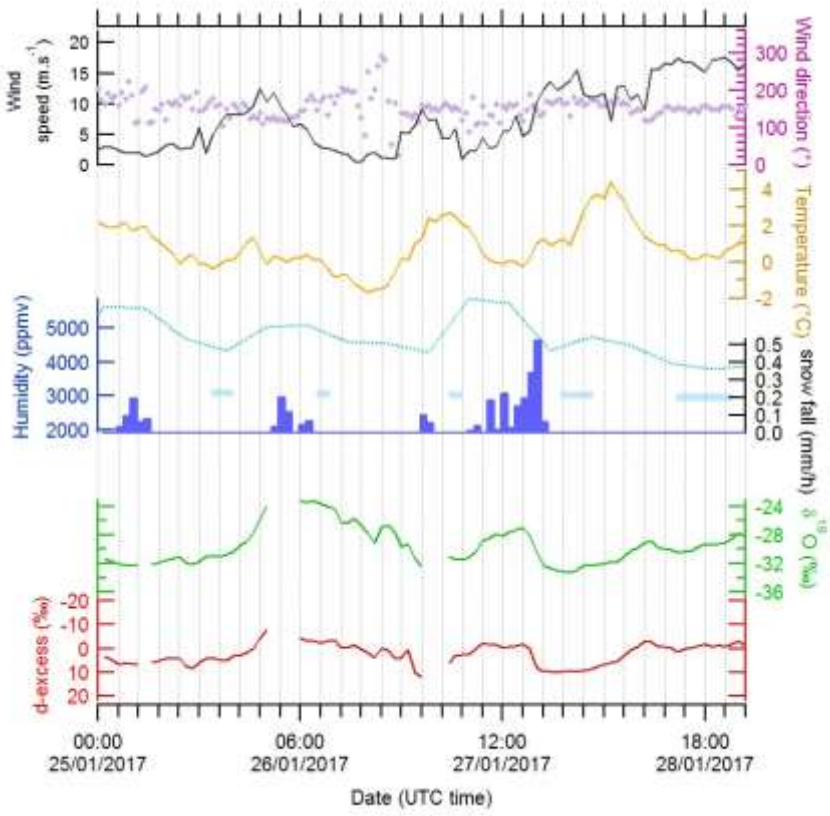

Figure 7*: Focus on the DDU weather and water isotopic data over the snow period. The wind direction, wind speed, temperature and humidity data are from the DDU weather station. The hourly snowfall rate and the presence of virga (horizontal light blue bars on the middle panel) are from Durán-Alarcón et al. (2018).*

Evolution of isotopic composition in this region may also arise from other processes, such as the influence of sublimation of blowing snow not taken into account in the MAR version of the model used here. Indeed, Barral et al. (2014) showed that sublimation of blowing snow affects vertical humidity profiles in Adélie land. Barral et al. (2014) evidenced a correlation between relative humidity of the low level of the atmosphere and katabatic wind speed at the windy plateau station D17. This is interpreted as an increase in sublimation of blowing snow during strong wind conditions. At DDU, the situation is however different. First, using our temperature and humidity records to calculate relative humidity, we show that the atmosphere is always undersaturated at DDU, except during snowfall events. Second, under clear sky conditions, diel cycles of relative humidity are anti-correlated with wind speed at DDU (similarly to the anti-correlation between specific humidity and wind speed observed in Figure 5a) in contrast with the positive correlation observed by Barral et al. (2014) at D17. Third, if sublimation of local blowing snow was a large source of surface vapor, then one would expect to observe a parallel increase of surface vapor $\delta^{18}O$ as snow is enriched in heavier isotopes compared to water vapor. In contrast, we observe an anti-correlation between $\delta^{18}O$ and wind speed (Figure 5a).

Finally, a comparison with the D3 (~ 1 km from Cap Prud'homme) and D17 (cf Figure 2) data for blowing snow (not available at DDU) shows that the flux of blowing snow is strong only at the end of the measurement period, beginning of February when the $\delta^{18}O$ values are not higher than for the rest of the period. Based on these lines of evidence, we conclude that diel variations in atmospheric dynamics and associated variations in transport of air masses from the plateau to the coast are better candidates to explain the $\delta^{18}O$ and d-excess diel cycles than diel variations in the sublimation of blowing snow at DDU. This may contrast with the situation on a coastal plateau station such as D17.

4-2- Comparison between DDU diel cycles and diel cycles at other polar locations

We now compare the occurrence, amplitude and characteristics of diel cycles in DDU isotopic records with other available records from polar regions. We explore whether there are systematic links between the characteristics of diel cycles in surface water vapor $\delta^{18}O$ and those in meteorological variables, as well as the relationships between diel isotopic cycles and geographic characteristics such as the distance to the open sea. Table 2 summarizes the characteristics of diel cycles observed in all available water vapor isotopic datasets to the authors' knowledge from Greenland and Antarctica. These records encompass summer seasons, most of them with documented snowfall events. At each site, diel cycles of temperature and humidity are identified most of the time. We thus calculated a characteristic diel cycle at each site through an average over a period of 5-7 consecutive days with unequivocal diel cycles of average amplitude. The smallest amplitudes of temperature diel cycles are observed in coastal regions of Antarctica (DDU and Syowa) as expected from the oceanic influence. Indeed, in coastal regions, the proximity of water is often associated with more cloudiness. In addition, the proximity of the ocean increases the proportion of latent heat flux and decreases the proportion of sensible heat flux with immediate consequences for the air temperature. The smallest amplitudes of the water vapor $\delta^{18}O$ and d-excess diel cycles are also observed at some coastal stations (Syowa, Ivittuut). Inland Antarctica, $\delta^{18}O$ diel cycles display amplitudes larger than 4.5‰; diel temperature variations are also large (larger than 8°C). There is however no systematic correspondence between the amplitude of the temperature diel cycle and the amplitude of the $\delta^{18}O$ diel cycle. This is particularly remarkable at DDU, where we observe a relatively small amplitude of temperature diel cycles (comparable to the other coastal stations in Antarctica), but an unusually large amplitude of the $\delta^{18}O$ diel variations (5.40 ‰ against 2.23 and 1.36 ‰ at the coastal locations of Syowa and Ivittuut). The relatively strong $\delta^{18}O$ diel variations observed at the coastal DDU station is in fact rather comparable to the one observed in the coastal station of Kangerlussuaq in summer 2011 (amplitude of $\delta^{18}O$ diel cycle of 3.51 ‰ to be compared to 1.36 ‰ at the Greenland coastal station of Ivittut). This pattern was attributed to the alternation between sea breeze and katabatic winds (Kopec et al., 2014).

		Dôme C[a]	Kohnen Station[b]	NEEM[c]	Ivittuut[d]	Syowa[e]	Kangerlussuaq[f]	**DDU[g]**
Temperature (°C)	Average value	-30.8	-23.4	-10.3	9.5	-1.9	10.0	**-0.5**
	Diel cycle amplitude	11.1	8.7	9.7	7.6	3.2	10.3	**4.5**
Humidity (ppmv)	Average value	600	1200	3100	11100	3900	7400	**3200**
	Diel cycle amplitude	500	1000	2100	1900	600	2200	**1300**
$\delta^{18}O$ (‰)	Average value	-68.94	-54.74	-43.83	-18.88	-28.12	-30.50	**-30.37**
	Diel cycle amplitude	6.48	4.87	3.01	1.36	2.23	3.51	**5.40**
d-excess (‰)	Average value	58	30	37	9	15	14	**3**
	Diel cycle amplitude	22	11	4	7	8	11	**10**
Period used for cycles characterization (days)		04/01/15 to 11/01/15	20/12/13 to 27/12/13	01/07/10 to 08/07/10	13/07/12 to 20/07/12	28/01/14 to 04/02/14	08/08/11 to 15/08/11	**Clear sky periods of this study**
Period of measurements (days)		25/12/14 to 17/01/15	17/12/13 to 01/01/14	24/05/10 to 29/07/10	01/07/12 to 31/07/12	20/01/14 to 09/02/14	21/07/11 to 15/08/11	**25/12/16 to 03/02/17**
Height of measurements (m)		2	0.2 – 3	0.1 – 1.5	5	1	1	**2**
Strong snowy period (days)		Not documented	19/12/12, 03/01/13, 07/01/13 and 17/01/13	28/06/10	Not documented	17/01/15 to 19/01/15	Not documented	**25/01/17 to 28/01/17**

373

374 *Table 2: Comparison of the diurnal evolutions of the climatic (temperature, humidity) and isotopic ($\delta^{18}O$, d-excess) parameters for different polar sites where*
375 *isotopic composition of water vapor is available.* [a]Casado et al., 2016*;* [b]Ritter et al., 2016*;* [c]Steen-Larsen et al., 2011*;* Steen-Larsen et al., 2013*;* [d]Bonne et
376 al., 2014*;* [e]Kurita et al., 2016a*,* Kurita et al., 2016b *;* [f]Kopec et al., 2014*;* [g] *This study*

377

At all sites exhibiting a diel cycle, the warmest hours are also associated with the highest humidity level and the highest $\delta^{18}O$ values. The link with wind speed is less systematic: higher wind speeds are observed during the warmest hours at Dome C, but during the coldest hours at DDU. A significant correlation is identified between $\delta^{18}O$ and temperature diel variations at most polar sites (DDU, Kohnen, Dome C, Ivittuut, Kangerlussuaq, NEEM), and for intra-seasonal variations in the absence of strong snow events at NEEM and Ivittuut, Greenland. At the diurnal scale, the $\delta^{18}O$ vs temperature slope is lower for continental sites (~ 0.6 ‰.°C^{-1} on average) than for coastal sites where isotopic diurnal cycles are clearly visible (i.e. Kangerlussuaq and DDU, 1.2 ‰.°C^{-1} on average). This confirms the similarities of the diel cycles identified in the short records available at Kangerlussuaq (25 days) and DDU (40 days), and motivates a detailed analysis of the water vapor isotopic variations on the two sites. We note that both records are hampered by calibration issues. No calibration of the isotopic data is presented for the Kangerlussuaq record, and we have reported the problems encountered with the standard delivery module at DDU and the resulting uncertainties.

The meteorological characteristics encountered during boreal summer 2011 in Kangerlussuaq and austral summer 2016-2017 in DDU reveals some similarities. Both exhibit a rather large amplitude of summer diel cycle for water vapor $\delta^{18}O$ in link with wind speed cycles. These two locations are affected by katabatic winds, stronger at DDU than at Kangerlussuaq (between 2 and 7 m.s^{-1} at Kangerlussuaq in Kopec et al. (2014), and between 0 and 20 m.s^{-1} at DDU in this study). Despite these similarities, local summer humidity levels are much lower at DDU than at Kangerlussuaq. This difference is first due to lower mean temperature at DDU. In addition, Kangerlussuaq is located in an alluvial flatland, near the confluence of two major regional rivers originating from the Russell Glacier, and its peak precipitation usually occurs in July-August. In summer 2016-2017, the presence of sea ice up to a distance of 70 km from DDU probably also contributed to our low humidity levels.

At Kangerlussuaq, the $\delta^{18}O$ and d-excess diel variations are explained by shifts in moisture origin, linked to local wind directions (Kopec et al., 2014). At night, continental winds bring relatively dry air with low $\delta^{18}O$ (high d-excess) of water vapor from the continent to the coastal station in the atmospheric boundary layer. During the day, due to increasing coastal land surface temperature, a sea breeze phenomenon occurs, bringing air masses with higher humidity levels of oceanic origin associated with high $\delta^{18}O$ (low d-excess). At DDU, we could not identify such a sea breeze phenomenon during summer 2016-2017 based on the wind data from DDU and the neighboring weather stations (Cap Prud'homme, D3, D17). The diel cycles may thus rather be triggered by variations in the intensity of continental winds, themselves related to diel temperature variations over the continent. The occurrence of a summer sea breeze phenomenon was clearly observed at DDU in earlier years (Pettré et al., 1993;

Jourdain, 2001; Angot et al., 2016). It may have been prevented by the particularly large sea ice extent during January 2017.

4-3- Sharp intra-daily isotopic variations and added value of water isotopes measurements

Finally, the fact that the impact of katabatic winds is also obvious in diel cycles of humidity and temperature questions the added value of measuring the isotopic composition of water vapor in addition to measurements of humidity only for the study of water cycle organization. Still, our record permits to identify at least one case in which continuous measurements of $\delta^{18}O$ and d-excess in the water vapor reveal an event not captured in the temperature and humidity series. We focus on a particular rapid event which occurred on December 28th, with a 3h sharp negative peak of $\delta^{18}O$ of 8.5 ‰ (with $\delta^{18}O$ values reaching -34 ‰), close to the amplitude of the average diel cycle (Figure 8). The associated d-excess increase is very strong and reaches 26 ‰, i.e. more than twice larger than the amplitude of the diel cycle during clear sky conditions. While the beginning of this remarkable isotopic excursion (decrease in $\delta^{18}O$ and increase in d-excess) corresponds to a decrease in humidity, hence probably an increase of arrival of dry air from the continent, the d-excess abrupt decrease and $\delta^{18}O$ abrupt increase 3 h later are in phase with abrupt change in the wind strength. This particular event shows the potential of water isotopes measurements to bring an added value on our knowledge of the atmospheric dynamics. It also shows that the atmospheric dynamics and associated wind characteristics should be considered for further interpretation of the water isotopic records in ice cores from coastal Adélie Land.

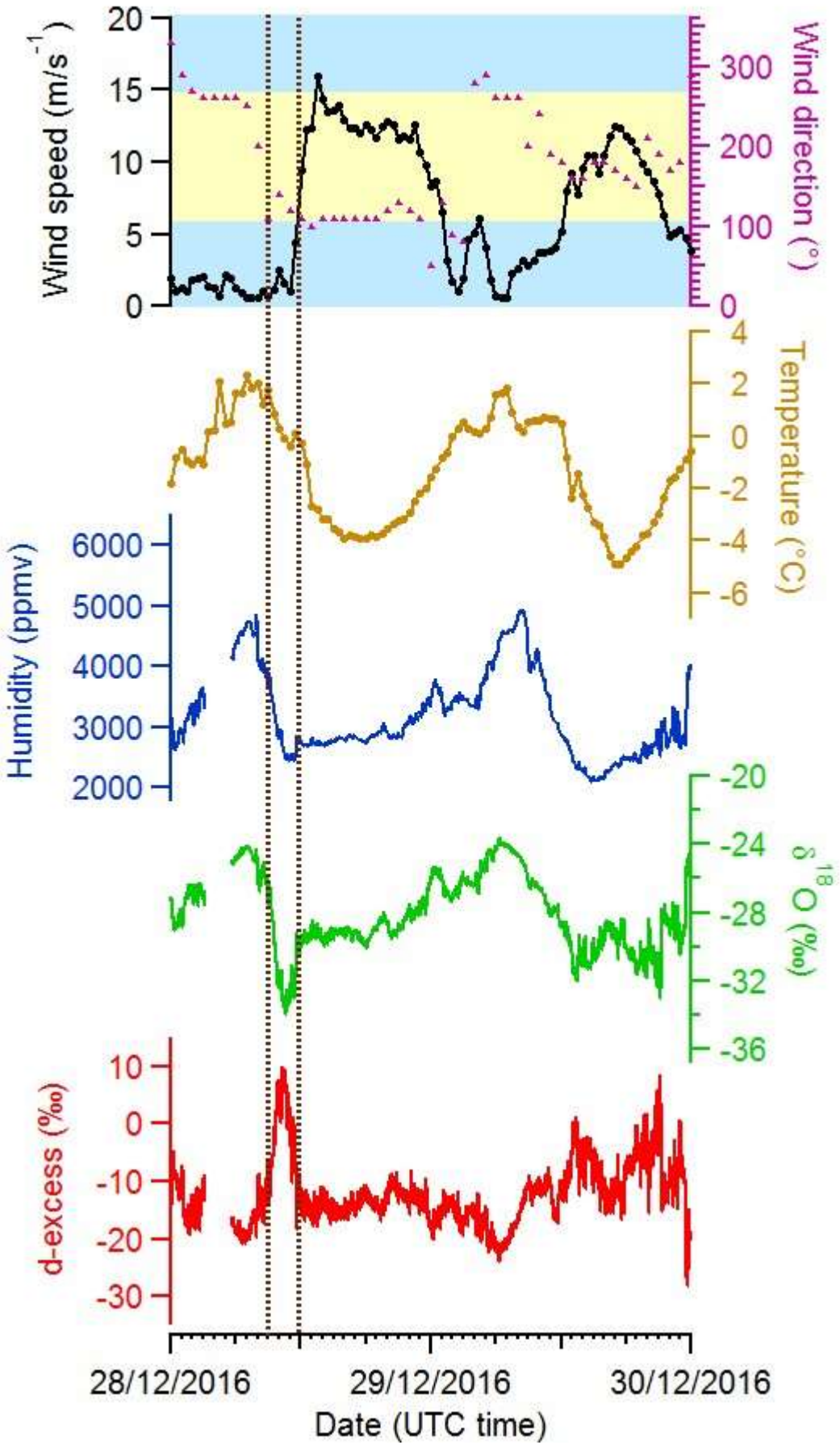
Wind speed (m/s^{-1})
20
15
10
5
0
Wind direction (°)
300
200
100
0
Temperature (°C)
4
2
0
-2
-4
-6
Humidity (ppmv)
6000
5000
4000
3000
2000
δ^{18}O (‰)
-20
-24
-28
-32
-36
d-excess (‰)
10
0
-10
-20
-30
28/12/2016
29/12/2016
30/12/2016
Date (UTC time)

431

Figure 8: Focus on a peak of $\delta^{18}O$ and d-excess (vertical dashed brown lines) on the 28th of December 2016. Wind strength and temperature data are from Cap Prud'homme to have a better temporal resolution (30 minutes)

5. Conclusion and perspectives

We presented the first water vapor isotopic record at the coastal station DDU in Adélie Land, a region strongly influenced by katabatic winds. During a 40-day measurement period, we evidenced clear and strong diel cycles especially during clear sky conditions. They can be explained by the occurrence of strong katabatic winds when continental temperature is low. During the coldest hours of the day, continental gravity winds increase downslope leading to enhanced arrival of low $\delta^{18}O$ and high d-excess in the water vapor at DDU. The comparison with available water vapor records in other polar sites supports close links between katabatic wind regimes and isotopic diel variations. Indeed, while diel cycles are not clearly seen in the water vapor isotopic composition of polar coastal sites of Ivittuut and Syowa, strong isotopic diel cycles are observed in the water vapor of the windiest coastal sites affected by diel variations of katabatic wind speed (Kangerlussuaq and DDU).

Since our water vapor isotopic record is longer at DDU than the one recorded at Kangerlussuaq, we are also able to highlight the added value of water isotopes with respect to humidity record for the study of water cycle in Adélie Land. In particular, short (~3 hours) peaks in $\delta^{18}O$ and d-excess as captured in our record correspond to abrupt changes in wind strength. This confirms that $\delta^{18}O$ of water vapor in coastal regions affected by katabatic winds is much more sensitive to air mass origins than e.g. to temperature or humidity. This finding has the potential to influence the interpretation of coastal ice core records in these regions (Goursaud et al., 2017).

The insights from our field campaign may not be fully representative of average conditions at DDU. One of the limits of our study is that sea ice did not break down at DDU during the 2016-2017 summer season, a rare but not unusual situation which very probably affected DDU weather conditions, including surface water vapor and its isotopic composition. Convection can also occur over an ocean free of ice leading to non-local mixing with the atmosphere above the boundary layer potentially affecting the isotopic composition. Obtaining longer records, including winter periods, is important to encompass a larger range of weather and climate conditions to further inform the interpretation of the isotopic records in Adélie Land.

Acknowledgments

The research leading to these results has received funding from the European Research Council under the European Union's Seventh Framework Programme (FP7/2007-2013) / ERC grant agreement n°

[306045]. We acknowledge the programs ASUMA and NIVO2 and the support of IPEV. Many thanks to Bruno Jourdain, Doris Thuillier and the technical staff at the Dumont d'Urville station in summer 2016-2017 for strong support. Support for this study was also obtained from the LEFE programs ADELISE and NEVE-CLIMAT as well as ANR ASUMA. Finally, we thank deeply Hans Christian Steen Larsen, Jean-Louis Bonne, Naoyuki Kurita, Ben Kopec and François Ritter for sharing the raw files of climate and isotopic data used for building Table 2.

References

Agosta, C., Amory, C., Kittel, C., Orsi, A., Favier, V., Gallée, H., van den Broeke, M. R., Lenaerts, J. T. M., van Wessem, J. M., van de Berg, W. J., and Fettweis, X. (2019) Estimation of the Antarctic surface mass balance using the regional climate model MAR (1979–2015) and identification of dominant processes, *The Cryosphere*, 13, 281-296, doi:10.5194/tc-13-281-2019.

Altnau, S., Schlosser, E., Isaksson, E., & Divine, D. (2015). Climatic signals from 76 shallow firn cores in Dronning Maud Land, East Antarctica. *The Cryosphere*, *9*, 925-944, https://doi.org/10.5194/tc-9-925-2015

Amory, C., Trouvilliez, A., Gallée, H., Favier, V., Naaim-Bouvet, F., Genthon, C., … Bellot, H. (2015). Comparison between observed and simulated aeolian snow mass fluxes in Adélie Land, East Antarctica. *The Cryosphere*, *9*(4), 1373–1383. http://doi.org/10.5194/tc-9-1373-2015

Angot, H., Dion, I., Vogel, N., Legrand, M., Magand, O., & Dommergue, A. (2016). Multi-year record of atmospheric mercury at Dumont d'Urville, East Antarctic coast: continental outflow and oceanic influences. *Atmospheric Chemistry and Physics*, *16*(13), 8265–8279.

Barral, H., Genthon, C., Trouvilliez, A., Brun, C., & Amory, C. (2014). Blowing snow in coastal Adélie Land, Antarctica: three atmospheric-moisture issues. *The Cryosphere*, *8*(5), 1905–1919.

Barral, H., Genthon, C., Trouvilliez, A., Brun, C., & Amory, C. (2014). Blowing snow in coastal Adélie Land, Antarctica: three atmospheric-moisture issues. *The Cryosphere*, *8*(5), 1905–1919. http://doi.org/10.5194/tc-8-1905-2014

Bindschadler, R., Vornberger, P., Fleming, A., Fox, A., Mullins, J., Binnie, D., … Gorodetzky, D. (2008). The Landsat image mosaic of Antarctica. *Remote Sensing of Environment*, *112*(12), 4214–4226.

Bonne, J.-L., Masson-Delmotte, V., Cattani, O., Delmotte, M., Risi, C., Sodemann, H., & Steen-Larsen, H. (2014). The isotopic composition of water vapour and precipitation in Ivittuut, southern Greenland. *Atmospheric Chemistry and Physics*, *14*(9), 4419–4439.

Casado, M., Landais, A., Masson-Delmotte, V., Genthon, C., Kerstel, E., Kassi, S., … Cermak, P. (2016). Continuous measurements of isotopic composition of water vapour on the East Antarctic Plateau. *Atmospheric Chemistry and Physics Discussions*, 1–26. http://doi.org/10.5194/acp-2016-8

Durán-Alarcón, C., Boudevillain, B., Genthon, C., Grazioli, J., Souverijns, N., Lipzig, N. P. M. Van, … Berne, A. (2018). The vertical structure of precipitation at two stations in East Antarctica derived from micro rain radars). *The Cryosphere, 13,* 247-264. https://doi.org/10.5194/tc-13-247-2019

Favier, V., Agosta, C., Genthon, C., Arnaud, L., Trouvillez, A., & Gallée, H. (2011). Modeling the mass and surface heat budgets in a coastal blue ice area of Adelie Land , Antarctica, *116*, 1–14. http://doi.org/10.1029/2010JF001939

Gallée, H., & Pettré, P. (1998). Dynamical constraints on katabatic wind cessation in Adélie Land, Antarctica. *Journal of the Atmospheric Sciences*, *55*(10), 1755–1770.

Garratt J. (1994). Review: the atmospheric boundary layer. *Earth-Science Reviews*, 37, 89–134. doi: 10.1016/0012-8252(94)90026-4

Goursaud, S., Masson-Delmotte, V., Favier, V., Preunkert, S., Fily, M., Gallée, H., … Minster, B. (2017). A 60-year ice-core record of regional climate from Adélie Land, coastal Antarctica. *The Cryosphere*, *11*(1), 343–362.

Goursaud, S., Masson-Delmotte, V., Favier, V., Preunkert, S., Fily, M., Gallée, H., … Werner, M. (2016). A sixty year ice-core record of regional climate from Adélie Land, coastal Antarctica. *The Cryosphere Discuss.*, *2016*, 1–36. http://doi.org/10.5194/tc-2016-179

Grazioli, J., Genthon, C., Boudevillain, B., Duran-Alarcon, C., Del Guasta, M., Jean-Baptiste, M., & Berne, A. (2017). Measurements of precipitation in Dumont d'Urville, Adélie Land, East Antarctica. *The Cryosphere*, *11*(4), 1797.

Jourdain, B. (2001). Etude du maillon atmosphérique du cycle biogéochimique du soufre aux hautes latitudes sud (station Dumont d'Urville).

Jouzel, J. (2013). *Water Stable Isotopes: Atmospheric Composition and Applications in Polar Ice Core Studies*. *Treatise on Geochemistry: Second Edition* (2nd ed., Vol. 5). Elsevier Ltd. http://doi.org/10.1016/B978-0-08-095975-7.00408-3

Jouzel, J., Delaygue, G., Landais, A., Masson-Delmotte, V., Risi, C., & Vimeux, F. (2013). Water isotopes as tools to document oceanic sources of precipitation. *Water Resources Research*, *49*(11). http://doi.org/10.1002/2013WR013508

König-Langlo, G., King, J., & Pettré, P. (1998). Climatology of the three coastal Antarctic stations Dumont d'Urville, Neumayer, and Halley. *Journal of Geophysical Research: Atmospheres*, *103*(D9), 10935–10946.

Kopec, B., Lauder, A., Posmentier, E., & Feng, X. (2014). The diel cycle of water vapor in west Greenland. *Journal of Geophysical Research: Atmospheres*, *119*(15), 9386–9399.

Kurita, N., Hirasawa, N., Koga, S., Matsushita, J., Steen-Larsen, H. C., Masson-Delmotte, V., & Fujiyoshi, Y. (2016a). Identification of Air Masses Responsible for Warm Events on the East Antarctic Coast. *SOLA*, *12*, 307–313.

Kurita, N., Hirasawa, N., Koga, S., Matsushita, J., Steen-Larsen, H. C., Masson-Delmotte, V., & Fujiyoshi, Y. (2016b). Influence of large-scale atmospheric circulation on marine air intrusion toward the East Antarctic coast. *Geophysical Research Letters*, *43*(17), 9298–9305. http://doi.org/10.1002/2016GL070246

Kusahara, K., Hasumi, H., Fraser, A. D., Aoki, S., Shimada, K., Williams, G. D., … Tamura, T. (2017). Modeling Ocean–Cryosphere Interactions off Adélie and George V Land, East Antarctica. *Journal of Climate*, *30*(1), 163–188.

Landais, A., Casado, M., Prié, F., Magand, O., Arnaud, L., Ekaykin, A., … Orsi, A. (2017). Surface studies of water isotopes in Antarctica for quantitative interpretation of deep ice core data. *Comptes Rendus - Geoscience*. http://doi.org/10.1016/j.crte.2017.05.003

Liu, H., Jezek, K., Li, B., & Zhao, Z. (2001). Radarsat Antarctic Mapping Project digital elevation model version 2. *Radarsat Antarctic Mapping Project Digital Elevation Model Version 2, Boulder, Colorado USA: National Snow and Ice Data Center. Digital Media.*

551 Marshall, G. J. (2003). Trends in the Southern Annular Mode from observations and reanalyses.
552 *Journal of Climate*, *16*(24), 4134–4143.

553 Massom, R. A., & Stammerjohn, S. E. (2010). Antarctic sea ice change and variability–physical and
554 ecological implications. *Polar Science*, *4*(2), 149–186.

555 Massom, R., Reid, P., Stammerjohn, S., Raymond, B., Fraser, A., & Ushio, S. (2013). Change and
556 variability in East Antarctic sea ice seasonality, 1979/80–2009/10. *PloS One*, *8*(5), e64756.

557 Masson-Delmotte, V., Hou, S., Ekaykin, A., Jouzel, J., Aristarain, A., Bernardo, R. T., … White, J. W. C.
558 (2008). A review of antarctic surface snow isotopic composition: Observations, atmospheric
559 circulation, and isotopic modeling. *Journal of Climate*, *21*(13), 3359–3387.
560 http://doi.org/10.1175/2007JCLI2139.1

561 Moore, M., Blossey, P.N., Muhlbauer, A., & Kuang, Z. (2016)? Microphysical controls on the isotopic
562 composition of wintertime orographic precipitation, *Journal of Geophysical Research:*
563 *Atmospheres*,121, 7235-7253. doi:10.1002/2015JD023763

564 Périard, C., & Pettré, P. (1993). Some aspects of the climatology of dumont D'Irville, adélie land,
565 Antarctica. *International Journal of Climatology*, *13*(3), 313–328.

566 Pettré, P., Payan, C., & Parish, T. R. (1993). Interaction of katabatic flow with local thermal effects in a
567 coastal region of Adelie Land, East Antarctica. *Journal of Geophysical Research: Atmospheres*,
568 *98*(D6), 10429–10440.

569 Ritter, F., Steen-larsen, H. C., Werner, M., Masson-delmotte, V., Orsi, A., Behrens, M., … Kipfstuhl, S.
570 (2016). Isotopic exchange on the diurnal scale between near-surface snow and lower
571 atmospheric water vapor at Kohnen station , East Antarctica, (February), 1–35.
572 http://doi.org/10.5194/tc-2016-4

573 Smith, J. A., Hillenbrand, C.-D., Kuhn, G., Larter, R. D., Graham, A. G., Ehrmann, W., … Forwick, M.
574 (2011). Deglacial history of the West Antarctic Ice Sheet in the western Amundsen Sea
575 embayment. *Quaternary Science Reviews*, *30*(5), 488–505.

576 Steen-Larsen, H. C., Johnsen, S. J., Masson-Delmotte, V., Stenni, B., Risi, C., Sodemann, H., … Ellehøj,
577 M. (2013). Continuous monitoring of summer surface water vapor isotopic composition above
578 the Greenland Ice Sheet. *Atmospheric Chemistry and Physics*, *13*(9), 4815–4828.

579 Steen-Larsen, H. C., Masson-Delmotte, V., Hirabayashi, M., Winkler, R., Satow, K., Prié, F., …
580 Sveinbjörnsdottír, A. E. (2014). What controls the isotopic composition of Greenland surface
581 snow? *Climate of the Past*, *10*(1), 377–392. http://doi.org/10.5194/cp-10-377-2014

582 Steen-Larsen, H. C., Masson-Delmotte, V., Sjolte, J., Johnsen, S. J., Vinther, B. M., Bréon, F.-M., …
583 White, J. (2011). Understanding the climatic signal in the water stable isotope records from the
584 NEEM shallow firn/ice cores in northwest Greenland. *Journal of Geophysical Research:*
585 *Atmospheres*, *116*(D6), n/a--n/a. http://doi.org/10.1029/2010JD014311

586 Stenni, B., Scarchilli, C., Masson-Delmotte, V., Schlosser, E., Ciardini, V., Dreossi, G., … others. (2016).
587 Three-year monitoring of stable isotopes of precipitation at Concordia Station, East Antarctica.
588 *The Cryosphere*, *10*(5), 2415.

589 Tamura, T., Ohshima, K. I., Fraser, A. D., & Williams, G. D. (2016). Sea ice production variability in
590 Antarctic coastal polynyas. *Journal of Geophysical Research: Oceans*, *121*(5), 2967–2979.

591 Thomas, E. R., van Wessem, J. M., Roberts, J., Isaksson, E., Schlosser, E., Fudge, T. J., … others. (2017).
592 Review of regional Antarctic snow accumulation over the past 1000 years. *Climate of the Past*
593 *Discussion*.

594 Titchner, H. A., & Rayner, N. A. (2014). The Met Office Hadley Centre sea ice and sea surface
595 temperature data set, version 2: 1. Sea ice concentrations. *Journal of Geophysical Research:*
596 *Atmospheres*, *119*(6), 2864–2889.

597 Touzeau, A., Landais, A., Stenni, B., Uemura, R., Fukui, K., Fujita, S., … Barkan, E. (2016). Acquisition of
598 isotopic composition for surface snow in East Antarctica and the links to climatic parameters.
599 *The Cryosphere*, *10*(2), 837–852.

600 Touzeau, A., Landais, A., Stenni, B., Uemura, R., Fukui, K., Fujita, S., … Risi, C. (2016). Acquisition of
601 isotopic composition for surface snow in East Antarctica and the links to climatic parameters.
602 *The Cryosphere*, *10*, 837–852. http://doi.org/10.5194/tc-10-837-2016

603 Tremoy, G., Vimeux, F., Mayaki, S., Souley, I., Cattani, O., Risi, C., … Oi, M. (2012). A 1-year longδ18O
604 record of water vapor in Niamey (Niger) reveals insightful atmospheric processes at different
605 timescales. *Geophysical Research Letters*, *39*(8).

606 Wendler, G., Stearns, C., Weidner, G., Dargaud, G., & Parish, T. (1997). On the extraordinary katabatic
607 winds of Adélie Land. *Journal of Geophysical Research: Atmospheres*, *102*(D4), 4463–4474.

608